Investigation of e-scooter drivers colliding with kerbs – a parametric numerical study

Patrick Matt, Marcin Jenerowicz, Timo Schweiger, Florian Heisch, Jörg Lienhard, Matthias Boljen

Abstract Most electric scooter-related injuries occur in single crashes and the reported use of helmets during accidents is very low. The objective of this study is to numerically investigate single e-scooter accidents at kerbs. A finite element (FE) model containing the THUMS AM50 V4.02, an e-scooter, a helmet, and a rigid kerbstone was created. The FE helmet model was parameterised by material characterisation and standard helmet tests and a new, unconventional helmet testing setup was proposed. In a parametric study using the FE solver LS-DYNA, collisions of the e-scooter rider against the kerb with three different velocities (10, 20, 30 km/h), two different impact angles (90°, 60°), and with and without the helmet were investigated. The accelerations at the head centre of gravity were measured and the injury criteria HIC, BrIC and CSDM were evaluated. The variation of the collision angle influenced the body-kinematics and the injury criteria values. Higher e-scooter collision speeds resulted in higher impact speeds and increased HIC. The wearing of a helmet was the main factor in the reduction of translational impact accelerations and HIC, while for BrIC and CSDM whether the values increased or decreased depended on the collision scenario.

Keywords e-scooter, FE analysis, helmet-modelling, human body model, injury criteria.

I. INTRODUCTION

Since the introduction of electric scooters (e-scooters) as a new mode of transportation and their rise in popularity, accidents and injuries have been reported globally [1-5]. Causes of e-scooter accidents include falls, collisions with objects, and being hit by a moving vehicle [1]. In a recent study by Stigson *et al.*, 82% of the reported injuries occurred in single crashes that did not involve another vehicle or person [3]. Besides e-scooter handling problems and falling due to no specific reason, a third of those accidents were caused by hitting a kerbstone (12–15%) and unfavourable surface features, e.g. low friction, potholes (21–22%) [3].

In Germany, the maximum speed of e-scooters is limited to 20 km/h and e-scooter riders must use bicycle lanes or, if no bicycle lanes are available, the road [4]. The wearing of a helmet is not mandatory. Similar regulations exist in Sweden [3].

Most of the reported injuries occur in the region of the head and face (28–44%) [1-4], the upper extremities (37–47%) [3-4] and the lower extremities (23–37%) [3-4]. Head injuries range from lacerations over fractures to traumatic brain injuries (TBI) [2][4]. In general, the documented use of helmets during accidents is very low, at 4–13% [1][3]. This raises the question to what extent the risk of sustaining head injuries could be reduced by wearing helmets, and if changes to infrastructure and modifications of e-scooters (e.g. bigger wheels) could also affect the safety of the e-scooter rider.

Insight into accident behaviour of e-scooter riders could be gained by using human body models (HBMs) [6]. HBMs in combination with finite element (FE) analysis have already been applied to investigate body-kinematics and injury risks for different types of vulnerable road user (VRU) in collisions [7-11].

Injury risks for HBM can be estimated by applying injury criteria, which link the probability of injury with a mechanical parameter. Well-known injury criteria for the head are the head injury criterion (HIC) [12], head impact power (HIP) [13], brain injury criterion (BrIC) [14], and cumulative strain damage measure (CSDM) [15]. The calculation of HIC is based on the translational resultant acceleration of the head centre of gravity (HCG) and exposure time. Translational accelerations are an important factor in causing skull fractures, but HIC does not

P. Matt (e-mail: patrick.matt@emi.fraunhofer.de; tel.: +497612714437) and M. Jenerowicz are Research Assistants and M. Boljen is Head of the Research Group *Human Body Dynamics* at Fraunhofer Institute for High-Speed Dynamics, Ernst-Mach-Institut, EMI, Freiburg, Germany. T. Schweiger is a Research Assistant, F. Heisch is a Master student and J. Lienhard is in charge of lightweight engineering in the group *Crash Safety and Damage Mechanics* at Fraunhofer Institute for Mechanics of Materials, IWM, Freiburg, Germany.

take into account the influence of rotational accelerations, which are an important factor in causing TBI [16]. In contrast to HIC, HIP considers translational and rotational accelerations at HCG, while BrIC is based on angular velocities at HCG. In comparison to the above-mentioned criteria, the CSDM is based on strain values and considers the deformation of the brain. The CSDM is predicted by determining the volume fraction of the brain exceeding a certain strain threshold.

The objective of this study is to numerically investigate single e-scooter accidents at kerbs using HBMs. The focus of this investigation is to evaluate the influence of different impact velocities (10, 20, 30 km/h) and angles (60, 90°), and also the effect of wearing a helmet on the outcome of kinematics, body-accelerations, and values of injury criteria (HIC, BrIC and CSDM).

II. METHODS

This section contains a brief introduction to the modelling components, the evaluation of kinematics and injury criteria, and the simulation matrix conducted for this parametric study.

Modelling components

The crash model built for this study consists of the following components: the e-scooter model, the helmet model, the HBM, and the sled system implementing the kerb and the ground.

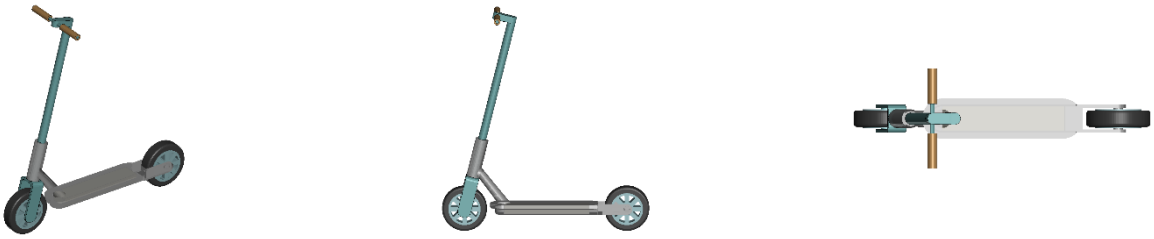

Scooter (iso) *Scooter (side)* *Scooter (top)*

Fig. 1. E-scooter FE model.

E-Scooter –The commercial Xiaomi M365 was chosen as a template for the e-scooter model. The final vehicle design has been designed by reverse engineering. Material models and constitutive parameters have been assigned by available data and best knowledge (Table I). The final model consists of roughly 62,000 nodes and 52,000 deformable elements and features rotating wheels, including solid rubber tyres, a free handlebar with soft deformable grips, and a massive component to represent the battery pack within the body part of the vehicle (Fig. 1).

TABLE I
VEHICLE SPECIFICATIONS

Specification	Mass	Length	Height	Width	Wheel diameter
Unit	kg	cm	cm	cm	inch
FE model	12.5	96.2	102.8	32.2	8.2

Helmet – Based on mechanical tests, the helmet model was parameterised and adjusted. From compression tests on foam plaques, stress-strain curves were used to model the material behaviour, and the strain rate dependence was assumed from literature [17-18]. In an e-scooter crash, different scenarios of head impact regarding impact angle and position are possible, which result in different loading conditions of the head and helmet. Instead of simple compression, this can lead to multiaxial loading. Therefore, to validate and adjust the model an unconventional test setup was developed. In Fig. 2, the testing concept is illustrated. This setup can be used to produce data with clearly defined boundary conditions. Compared to real e-scooter tests with dummies or collision simulations with HBMs, the focus of this experimental setup lies on the investigation of the helmet model. For the helmet mounting, a head-form with standard measures, with a circumference of 560 mm according to DIN EN 1078 [19], was manufactured out of acrylonitrile butadiene styrene (ABS) by fused deposition

modelling (FDM). A core pin made of steel, with a diameter of 90 mm, was mounted central in the 3D printed head-form. In contrast to the head recommended in DIN EN 1078, the diameter of the core pin was chosen so that the elasticity of the head in this experiment is comparable to that of the HBM's head (details below). At the lower end of the pin, a flange and a rectangular mounting enabled rotation around the axis, while the construction could be fastened with M16 screws. During the test, no movement of the mounted head was observed. According to the impact angles from previous crash simulations, three different scenarios were selected by changing the angles α and β (Fig. 2A). A total of nine helmet tests with and without polycarbonate (PC) shells were performed with reproduceable results. In Fig. 2B, the printed head-form and its mounting in a drop tower (IMATEK IM 10T-15) are shown. Figure 2C shows the testing setup with an impact mass of 7.7 kg and an impact velocity of 5 m/s. A piezo-sensor (Kistler 40 kN) and two high-speed cameras were used to measure the 3D-deformation of the speckled helmet by using digital image correlation (DIC). The movement of the flat impactor was measured with an integrated magnet-sensor.

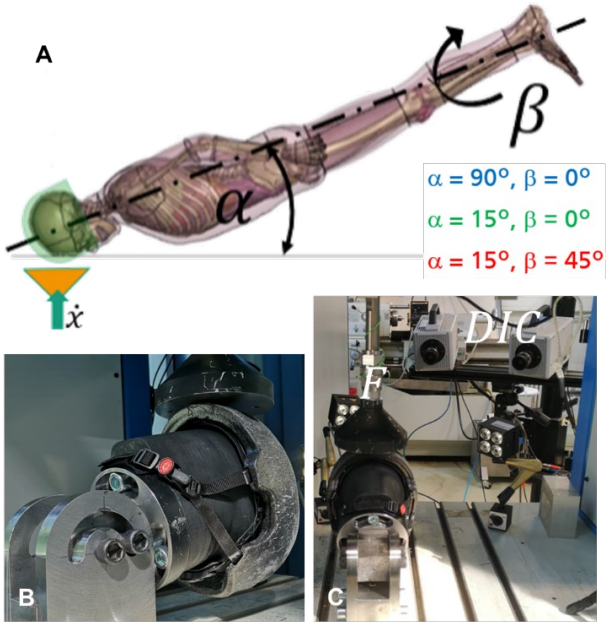

Fig. 2. Concept of realistic scenario helmet testing.
A – Definition of impact angles. B – Head model mounted in a two-axis rotation construction. C – Test setup of drop tower testing.

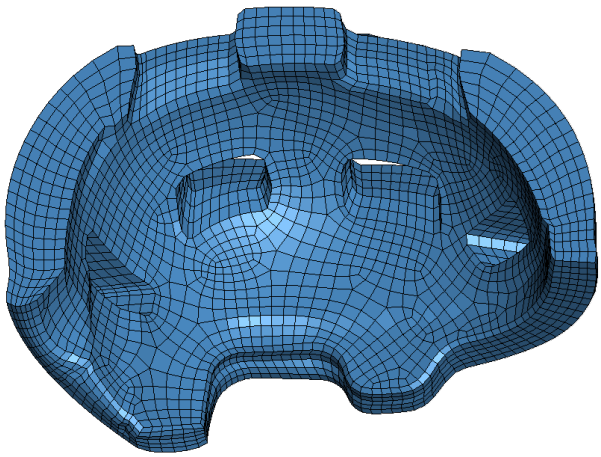

Fig. 3. Half helmet model for the FE-simulations

The FE model of the helmet was created from a CAD model featuring the helmet design. Thus, several constructional details had to be simplified to maintain a medium element size of 3 mm, as the main part, the inner foam, was built up from hexahedron elements to avoid any numerical inaccuracies, with a total number of 15,000 elements (Fig. 3). The helmet has a thin layer of PC on the outside. This layer was modelled with quadric shell elements sharing nodes with the inner volume elements. Thereby, no contact had to be introduced, and it was assumed that no delamination occurred during the loading of the helmet. The chinstrap, keeping the helmet on the HBM during the crash, was also modelled with shell elements.

For simulating the material behaviour of the foam, the widely used model *MAT_FU_CHANG_FOAM was employed and parameterised by the compression experiments mentioned above. Supplementary material regarding the stress strain curves of the foam can be found in the appendix. A standard *MAT_PIECEWISE_LINEAR_PLASTICITY model was appointed for the PC layer with parameters from literature [20].

The 3D printed head-form and its steel core were modelled linearly elastically. Its stiffness was compared to that of a THUMS head, showing similar behaviour (Fig. 4). However, in the simulations of the helmet tests, it was observed that the stiffness had little influence and could also be modelled as rigid without significantly changing the forces.

Three impact configurations of the helmet testing (Fig. 2A) were simulated in good agreement with the experimental results. Exemplarily, the force-displacement-curves of the test with α = 15° and β = 45° are displayed

in Fig. 5. Additionally, the normal setup (coloured in blue), experiments and simulations were then performed with the PC layer removed, thereby purely testing the foam (red). In both cases, the numerical predictions are well in accord with real-world observations. The overall stiffnesses are in line, as well as the absorbed energy.

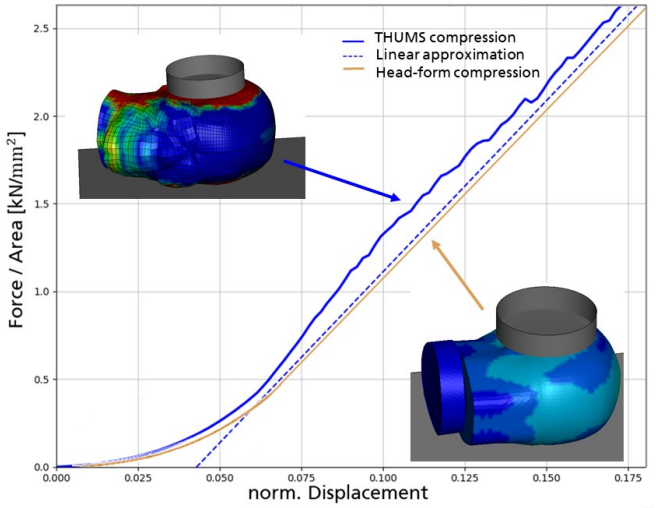

Fig. 4. Numerical testing of the lateral stiffness under compression with THUMS model and the head-form.

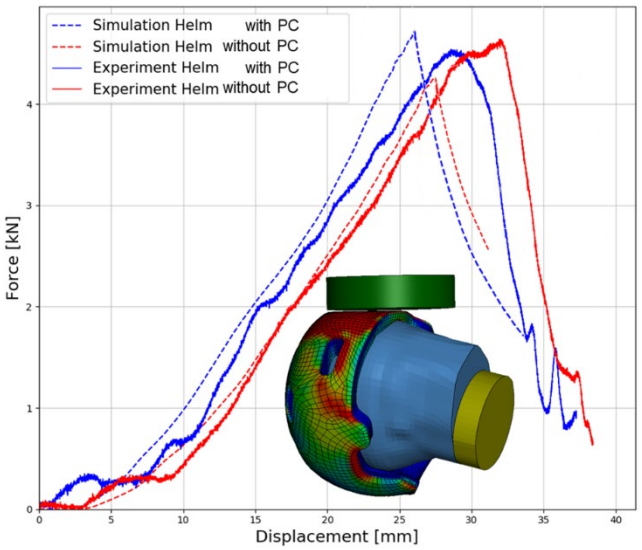

Fig. 5. Experiments (solid lines) and simulations (dashed lines) of the helmet impact test with rotation angels α = 15° and β = 45°, including the PC layer (blue) and excluding it (red).

Human Body Model – For the representation of the e-scooter rider, the 50th percentile male THUMS AM50 Pedestrian Model Version 4.02 [21] was chosen. The posture of the pedestrian was changed in a pre-positioning simulation into a riding stance by moving the feet into a tandem-style position [22] with the hands on top of the grips of the scooter. In order to evaluate the kinematics and injury criteria, a sensor was implemented in HCG by using *CONSTRAINED_INTERPOLATION according to Euro NCAP [23]. A local coordinate system was defined for this sensor. Attaching the helmet to the rider was realised with a *CONTACT_AUTOMATIC_SURFACE_TO_SURFACE definition and an additional chinstrap. Figure 6 displays the positioned THUMS with equipped helmet.

Before colliding with the kerbstone, the rider and the scooter were preloaded with gravitational loading for 54 ms, to establish a specific contact force of 0.75 kN between the two. To prevent the slipping of the extremities during the preload phase, the friction coefficient between THUMS and scooter was set to 0.5.

Fig. 6. Positioned THUMS on e-scooter with helmet: feet in tandem-style and hands on grips.

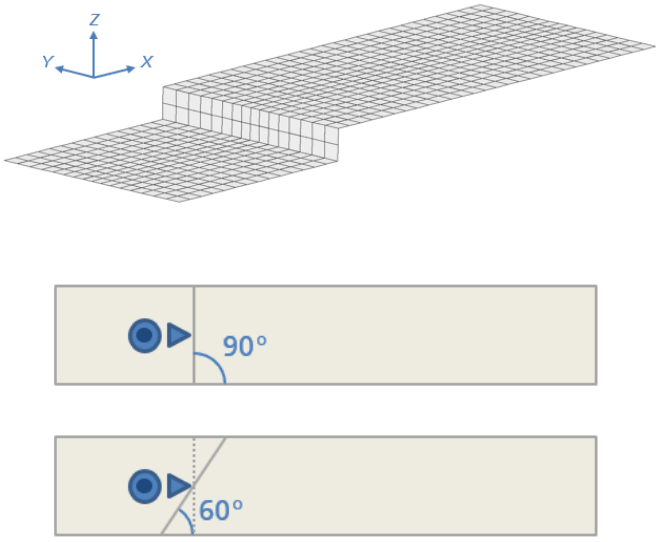

Fig. 7. Sled model and setup of scooter-driver. Kerb angles with respect to direction of movement.

Sled model – The kerb and the ground have been modelled by a simple shell model consisting of two finite planes of different height in Z direction. The model can be used in two modes: either fixed in space (for modelling a normal crash when the scooter is moving, as in this study); or as an impactor by moving it linearly along X direction (for modelling an inverse crash against the standing scooter). The kerb and the ground are fully customizable with respect to the length dimensions, the mesh size, the mesh bias and the kerb angle. The setup used for this study is as follows: 10 cm kerb height, 120 cm sled width, 150 cm sled length before kerb, 650 cm sled length after kerb. The model is set up by roughly 4,000 rigid elements and 4,000 nodes. Figure 7 illustrates the sled model and the collision angles.

Evaluation of kinematics and injury criteria

For the investigation of the accident behaviour of the e-scooter rider, the kinematics and several injury criteria were evaluated.

Kinematics: a qualitative observation of the body-kinematics of the HBM during the collisions was conducted. Furthermore, the resultant peak values of linear and angular accelerations and velocities at HCG were determined.

Injury Criteria: due to the fact that most injuries were reported in the region of the face and head, and the lack of criteria for the extremities, the injury assessment focused on head injury criteria. Therefore, HIC_{15}, BrIC and CSDM were evaluated. For the CSDM, a critical strain threshold of 15% was chosen ($CSDM_{15}$) because of the fact that in the original study [15] the best correlation was observed at a strain value of 15%.

Simulation Matrix

All simulations were conducted with LS-DYNA version 12. The total simulation time amounted to 860 ms, including the 54 ms pre-loading phase.

To ensure that the simulations with HBM and helmet would not terminate due to negative volume errors, the erosion of elements with negative volume was activated. This step had to be taken because of the high computation time and late head impact, which made the adaptation of the helmet parameters very costly. The volume of the eroded elements in the helmet ranged from 0.7% to 2.1%, which was an acceptable fraction. A typical case of eroded helmet elements can be found in the appendix.

For each simulation a different combination of collision angle (60, 90°) and velocity (10, 20, 30 km/h), and status of protection (with or without helmet) was chosen (Table II). A velocity of 20 km/h was chosen to represent the legal speed limit in Germany and 10 and 30 km/h to investigate significantly lower and higher accident speeds.

TABLE II
SIMULATION PARAMETERS

Scenario	Angle [°]	Velocity [km/h]	Helmet	Scenario	Angle [°]	Velocity [km/h]	Helmet
60_10_wo	60	10	No	60_10_w	60	10	Yes
90_10_wo	90	10	No	90_10_w	90	10	Yes
60_20_wo	60	20	No	60_20_w	60	20	Yes
90_20_wo	90	20	No	90_20_w	90	20	Yes
60_30_wo	60	30	No	60_30_w	60	30	Yes
90_30_wo	90	30	No	90_30_w	90	30	Yes

III. RESULTS

Analysis of Kinematics

In general, all collisions followed a similar pattern (Fig. 8 and Fig. 9). When the e-scooter collided with the kerbstone, the front wheel was blocked. For a collision angle of 60° the scooter skidded along the kerb, while for an angle of 90° and in *60_10_wo* and in *60_10_w* the backend was levered upwards. The levering upwards of the scooter resulted in a higher displacement of the lower limbs, which could not be observed in the skidding cases (Fig. 8 and Fig. 9 at t = 250 ms). During the first milliseconds after colliding with the kerb, the hands of the THUMS slid off the grips and the rider was either thrown past (60°) or over (90°) the handlebar. In mid-air, the arms were

outstretched in front of the body due to inertia. As soon as the hands came into contact with the ground, the arms were pushed, with seemingly no resistance, back to the side of the body due to the lack of muscle tension. In most cases the THUMS hit the ground head-first (Table III), not taking the hand contact into account. In the 20 km/h and 30 km/h scenarios with an angle of 60° the THUMS impacted the ground with the lower body first, but shortly after followed by the head. In these cases, the resultant velocities of the head impact were even higher compared to the 90° simulations (Table III). The forehead, unprotected without a helmet or protected with a helmet, was the region of the head that primarily hit the ground in the initial impact. The face (maxilla, mandible) secondarily impacted the ground.

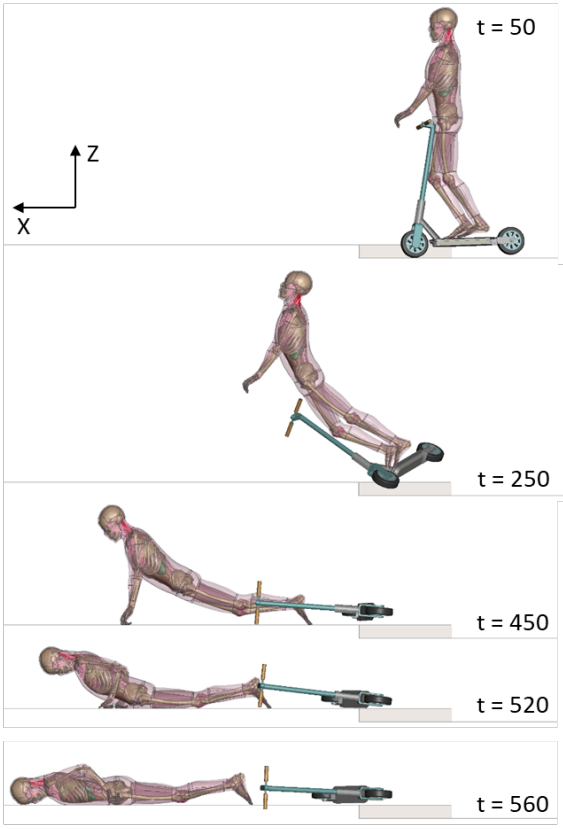

Fig. 8. Crash behaviour for 60°, 20 km/h and without helmet (time in ms).

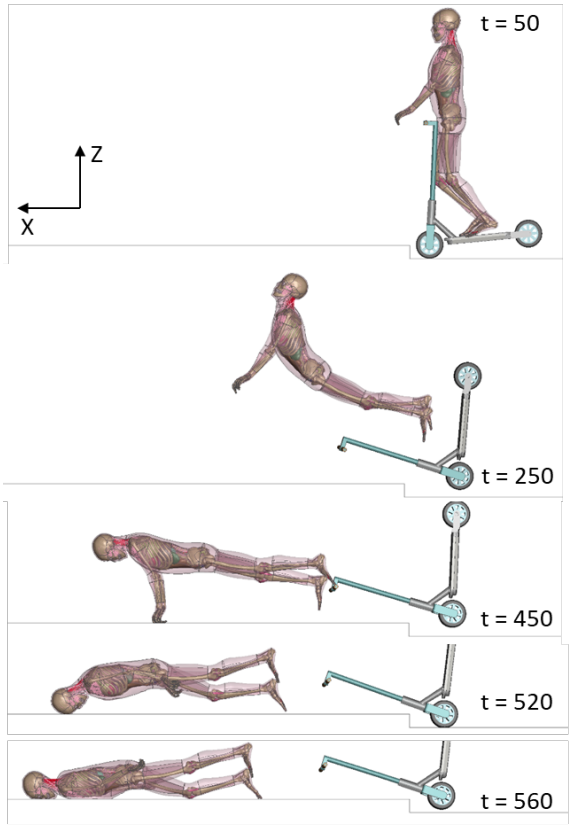

Fig. 9. Crash behaviour for 90°, 20 km/h and without helmet (time in ms).

TABLE III

SUMMARIZATION OF HEAD OR LOWER BODY (LB) FIRST IMPACTING THE GROUND, AND RESULTANT PEAK VELOCITY (V), ACCELERATION (A), ANGULAR VELOCITY (V_ANG) AND ANGULAR ACCELERATION (A_ANG) OF THE HEAD DURING GROUND IMPACT

Scenario	Part	v [m/s]	a [g]	v_ang [rad/s]	a_ang [rad/s²]
60_10_wo	Head	5.35	423	44.2	21100
90_10_wo	Head	5.73	355	49.3	20500
60_20_wo	LB	8.34	464	43.3	35300
90_20_wo	Head	7.04	409	40.9	27400
60_30_wo	LB	10.10	494	48.0	37600
90_30_wo	Head	9.25	488	41.9	25900
60_10_w	Head	5.36	120	33.0	10900
90_10_w	Head	5.65	173	55.9	8150
60_20_w	LB	8.28	204	53.1	18700
90_20_w	Head	7.21	170	38.3	9710
60_30_w	LB	10.60	534	59.3	54500
90_30_w	Head	8.89	223	40.0	33900

The head of the THUMS hit the ground after 470–740 ms (Fig. 10) and the body continued to slide over the ground (Fig. 11). Higher collision speeds and an angle of 90° resulted in earlier head impacts. The distance of the first head impact was mainly influenced by the velocity and ranged from 2.1 m to 4.8 m (Fig. 11). The presence of the helmet had no significant influence on the outcome of impact time and distance.

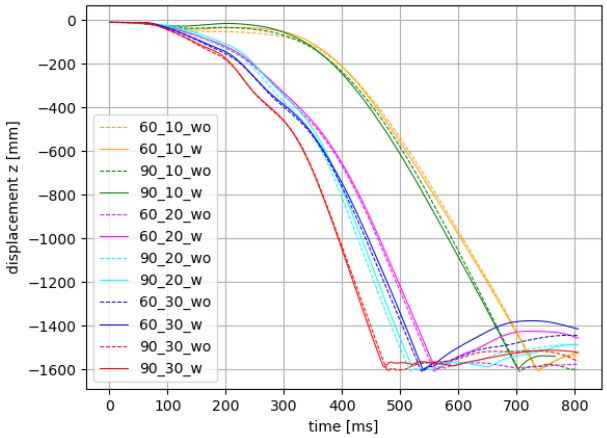

Fig. 10. z-displacement of HCG over time (combination of 60°, 90°; 10, 20, 30 km/h; with, without helmet).

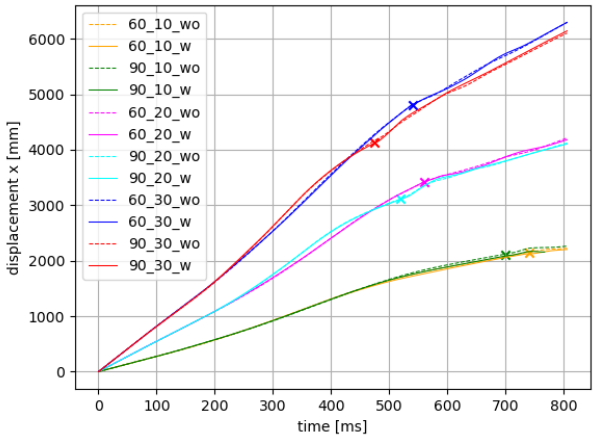

Fig. 11. x-displacement of HCG over time (combination of 60°, 90°; 10, 20, 30 km/h; with, without helmet). Symbol x indicates first contact of the head with the ground.

The head hit the ground with a resultant velocity of 5.52 ± 0.17 m/s (e-scooter collision speed: 2.78 m/s), 7.72 ± 0.60 m/s (e-scooter collision speed: 5.56 m/s) and 9.71 ± 0.68 m/s (e-scooter collision speed: 8.3 m/s) (Table III). For most cases, higher e-scooter collision velocities and an impact angle of 60° resulted in increased kinematic peak values (Table III). In nearly all simulations with a helmet compared to the simulations without, a reduction of the resultant linear peak acceleration of 51–72% could be seen (Fig. 12). An exception was *60_30_w*, in which a higher peak could be observed compared to *60_30_wo*. The resultant angular peak acceleration was reduced by 47–65% by the helmet for *60_10_w*, *90_10_w*, *60_20_w*, *90_20_w*, while for *60_30_w* and *90_30_w* an increase of 31–45% was observed (Fig. 13). More details regarding the accelerations and velocities at the HCG and kinetic energy profiles (20 km/h, without helmet) are provided in the appendix.

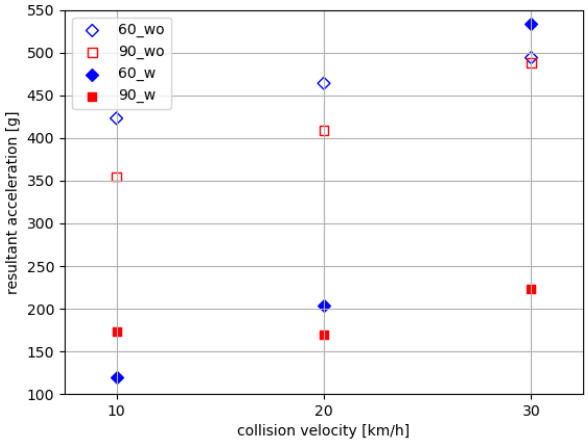

Fig. 12. Resultant linear acceleration of HCG over e-scooter collision velocity during ground impact (60° or 90° collision angle and with or without helmet).

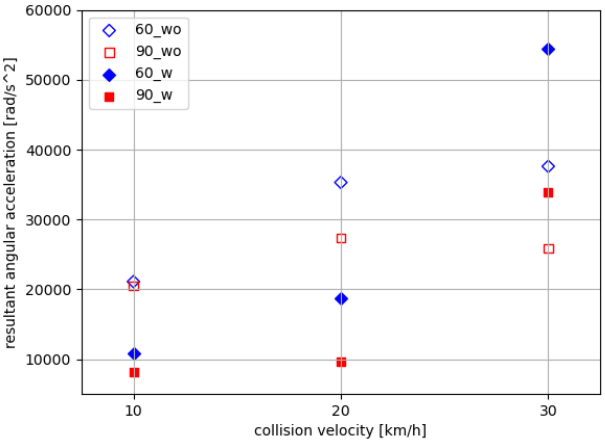

Fig. 13. Resultant angular acceleration of HCG over e-scooter collision velocity during ground impact (60° or 90° collision angle and with or without helmet).

Analysis of Injury Criteria

The predicted HIC values ranging from 319 to 6644 are shown in Fig. 14. It is clear that a reduction of collision velocity resulted in lower HIC. Comparing the scenarios regarding the status of protection, the addition of the

helmet decreased HIC between 70% and 91%, not taking *60_30_w* into account. In *60_30_w*, HIC was reduced by 33%. The variation of the collision angle also had a noticeable effect on the measured values. Without a helmet, the 90° HIC values were lower compared to 60°, while with a helmet the 90° HIC values were higher. According to Prasad and Mertz [24], a HIC of approximately 1450 is equivalent to a 50% risk of sustaining a skull fracture. This level has been exceeded by all scenarios without a helmet.

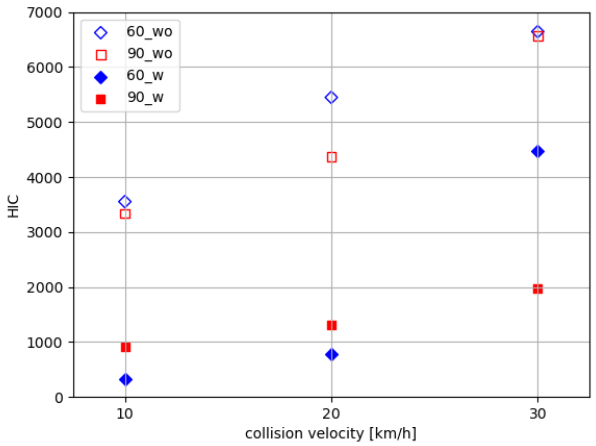

Fig. 14. HIC over e-scooter collision velocity (60° or 90° collision angle and with or without helmet).

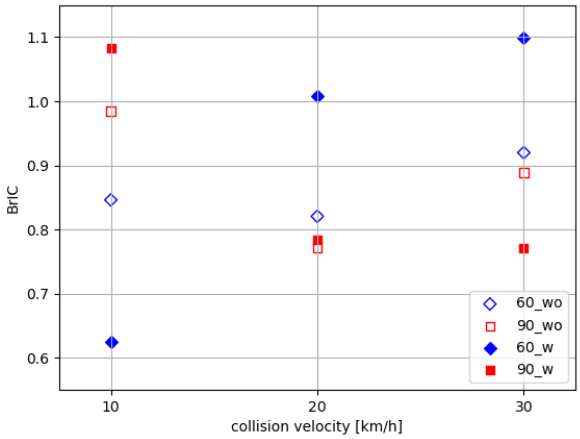

Fig. 15. BrIC over e-scooter collision velocity (60° or 90° collision angle and with or without helmet).

In contrast to HIC, the predicted BrIC showed no clear correlation either with velocity or with collision angle (Fig. 15). The lowest value was predicted with 0.626 for *60_10_w* and the highest value of 1.098 for *60_30_w*. In four of six cases, the addition of the helmet led to an increase of BrIC. A BrIC of 1.06 marks the 50% threshold of sustaining an AIS4 head injury [14]. Except for *90_10_w* and *60_30_w*, all predicted values are below 1.06.

The $CSDM_{15}$ are illustrated in Fig. 16. Overall, all predicted results are very high, showing that 87% up to 98% of all brain volumes have exceeded the strain threshold of 15%. A decrease of velocity tends to decrease the $CSDM_{15}$ slightly, except for *90_10_wo* and *90_10_w*. In four cases, the helmet reduced the values, while in both 30 km/h scenarios the presence of the helmet resulted in a slight increase. According to Takhounts *et al.* [15], a $CSDM_{15}$ of 55% is equivalent to a 50% risk of sustaining an AIS4+ head injury, which has been exceeded by every predicted value.

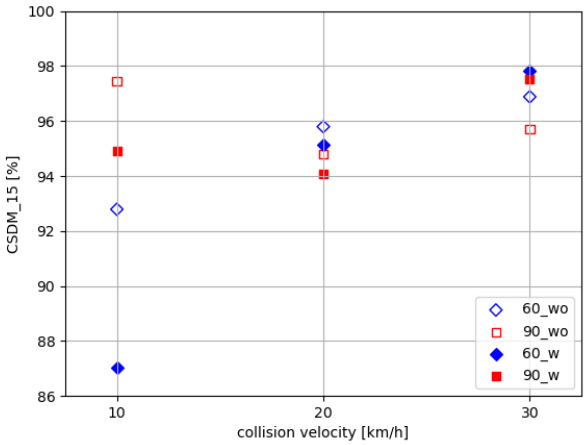

Fig. 16. $CSDM_{15}$ over e-scooter collision velocity (60° or 90° collision angle and with or without helmet).

IV. DISCUSSION

In the following section the helmet testing and modelling, the effect of the parametric variation on crash outcome, and the limitations of this study will be discussed.

Helmet Testing and Modelling

A wide range of crash scenarios exists. The e-scooter kerb accident is a commonly reported real-life accident scenario. Depending on the angle and velocity of the e-scooter impact on the kerb, the human body hits the ground with numerous different angles and impact velocities. To predict the impact forces on the head with helmets, the helmet model needs adjustments beyond scenarios defined in DIN EN 1078 [19]. The multiaxial loading should be validated in realistic helmet impact scenarios. Therefore, the unconventional testing setup is recommended (Fig. 2). Two rotational degrees of freedom of the testing head allowed the adjustment of all impact angles that were predicted in crash simulations. The helmet model has been adjusted with these realistic scenarios and is in accordance with the experiment (Fig. 5). Parameterisation with compression data alone may not fit the reaction forces correctly.

Aside from collision angle and loading triaxialities, different test velocities must also be considered. As shown, ground impact velocities are higher (Table III) than the recommended values of 4.57 m/s and 5.42 m/s in the standard-testing of DIN EN 1078. Underestimating the impact speed in helmet testing could be a potential safety risk. Thus, regulations for helmet and other protectors testing should be adjusted to reflect more closely real crash scenarios.

Further work in modelling helmets should also focus on the strain rate-dependent damage behaviour. Simple stress threshold defined element erosion cannot sufficiently predict the after-fracture initiation behaviour. Furthermore, the numerical helmet stability should be improved to avoid element erosion due to negative volumes. However, as mentioned above, the eroded volume fraction was in an acceptable range, and should therefore have a tolerable effect on the predicted values for this study.

Effect of parameter variation

The variation of the collision angle influenced the accident characteristics of e-scooter and HBM. In all 90° simulations, a scooter leverage effect could be seen, which caused a tossing upwards of the lower body, and then the THUMS hitting the ground head-first, instead of lower body first. Therefore, one would expect higher impact velocities, but contrary to expectation these were observed in the 60° scenarios, in which, for most cases, the lower body hit the ground first, followed by the head. An explanation could be that the process of the head's backwards and forwards motion is completed earlier in the 90° scenario (Fig. 9), so that the head is already slowed down before it actually hits the ground, which could have resulted in decreased impact velocities and accelerations (Table III). The collision angles also had a noticeable effect on the predicted injury criteria values, but no clear pattern could be observed. Investigating a wider range of angles could provide more insight.

Higher e-scooter collision speeds against the kerbstone resulted in increased ground-impact speeds. Similar results were reported by Posirisuk *et al*., who investigated e-scooter falls with multi-body dynamic models of an e-scooter and different riders [6]. Furthermore, higher collision speeds also led to an increase of resultant peak accelerations at HCG during ground impact, and therefore increased HIC values. In most cases the CSDM showed a slight increase with increasing e-scooter collision velocity, while no clear correlation between BrIC and collision velocity could be observed.

The helmet had a significant effect on the outcome of reducing the linear resultant peak acceleration and HIC, as also reported by [7][11][25-26], which are both often associated with skull fracture [16][24]. In the case of *60_30_w*, an increase of resultant peak acceleration was observed when wearing a helmet. This seems to be an anomalous value in comparison to the other values.

In contrast to HIC predictions, the addition of the helmet resulted in increased BrIC values in four of six cases, and the $CSDM_{15}$ was mostly reduced just slightly with the helmet. In the two 30 km/h scenarios, the wearing of a helmet caused higher $CSDM_{15}$, as was the case for most BrIC values. Wang *et al*. reported similar findings for BrIC and $CSDM_{25}$ in a bicycle-kerb impact scenario, while for a skidding impact scenario the helmet reduced the $CSDM_{25}$ noticeably [7].

Limitations and Outlook

A limitation of this study is that the effect of muscle tension [27-28] and active movement could not be considered. Thus, it should be emphasised that the kinematics of the THUMS described above represent the behaviour of a model without muscle activity. It can be assumed that muscle activation would have led to a different outcome in kinematics and therefore, the predicted HBM-kinematics should not be seen as real-life

behaviour. Due to this limitation, real-life crash behaviour, which would include holding onto the handlebar, trying to break the fall and protecting the head, could not be modelled, and hence could not be considered in the prediction of the injury criteria values. These restrictions could lead to an overestimation of predicted injury values. Moreover, this work is limited to the results obtained by the 50th percentile male THUMS, thus currently not taking females and other percentiles into account.

Nonetheless, the study shows a tendency that a speed reduction, and especially the wearing of a helmet, decreases linear accelerations at HCG during ground impact and HIC values.

For future studies the effect of attempting to break the HBM's fall on the outcome of injury criteria values, and also the effect of applying additional protective equipment [29] on predicted injury risks for arms and legs, which are also often injured in e-scooter falls, could be investigated.

Furthermore, the performance of the helmet design could be enhanced by investigating different materials numerically. In particular, the potential of micro-structured materials with a stiffness gradient could be explored [30]. Even though features on such a small scale cannot be modelled in an e-scooter accident directly, the application of surrogate material models would make these investigations possible.

V. CONCLUSIONS

In this study single e-scooter accidents at kerbs were analysed numerically with HBM. A FE model, containing the THUMS AM50 V4.02, an e-scooter, a helmet and a rigid kerbstone, was created. The FE helmet model was parameterised by material characterisation and standard helmet tests. More realistic helmet impact scenarios were proposed and tested. In the HBM single e-scooter accidents the effect of collision angle, collision velocity and the wearing of a helmet on the outcome of body-kinematics and injury criteria values were determined. The variation of the collision angle influenced the body-kinematics and injury criteria values. Higher e-scooter collision speeds resulted in higher impact speeds and increased HIC values. The wearing of a helmet reduced the translational impact accelerations and HIC values, significantly, while for BrIC and CSDM, whether the values increased or decreased depended on the scenario.

VI. ACKNOWLEDGEMENTS

The authors would like to acknowledge the support of the Sustainability Center Freiburg, Germany. The authors would also like to thank UVEX SPORTS GROUP GmbH & Co. KG, Germany, for providing samples and helmets.

VII. REFERENCES

[1] Trivedi, T. K., Liu, C., *et al*. (2019) Injuries Associated With Standing Electric Scooter Use. *JAMA Network Open*, **2**(1): p.e187381.

[2] Brownson, A. B., Fagan, P. V., Dickson, S., Civil, I. D. (2019) Electric scooter injuries at Auckland City Hospital. *New Zealand Medical Journal*, **132**(1505): pp.62–72.

[3] Stigson, H., Malakuti, I., Klingegård, M. (2021) Electric scooters accidents: analyses of two Swedish accident data sets. *Accident Analysis & Prevention*, **163**: p.106466.

[4] Störmann, P., Klug, A., *et al*. (2020) Characteristics and injury patterns in electric-scooter related accidents—a prospective two-center report from Germany. *Journal of Clinical Medicine*, **9**(5): p.1569.

[5] Liew, Y. K., Wee, C. P. J., Pek, J. H. (2020) New peril on our roads: a retrospective study of electric scooter-related injuries. *Singapore Medical Journal*, **61**(2): p.92.

[6] Posirisuk, P., Baker, C., Ghajari, M. (2022) Computational prediction of head-ground impact kinematics in e-scooter falls. *Accident Analysis & Prevention*, **167**: p.106567.

[7] Wang, F., Wu, J., *et al*. (2022) Evaluation of the head protection effectiveness of cyclist helmets using full-scale computational biomechanics modelling of cycling accidents. *Journal of Safety Research*, **80**: pp.109–134.

[8] Shi, L., Han, Y., Huang, H., Davidsson, J., Thomson, R. (2020) Evaluation of injury thresholds for predicting severe head injuries in vulnerable road users resulting from ground impact via detailed accident reconstructions. *Biomechanics and Modeling in Mechanobiology*, **19**(5): pp.1845–1863.

[9] Shang, S., Zheng, Y., Shen, M., Yang, X., Xu, J. (2018) Numerical investigation on head and brain injuries caused by windshield impact on riders using electric self-balancing scooters. *Applied Bionics and Biomechanics*, p. 5738090.

[10] Kofler, D., Tomasch, E., Spitzer, P., Klug, C. (2020) Analysis of the Effect of Different Helmet Types and Conditions in Two Real-world Accident Scenarios with a Human Body Model. *Proceedings of IRCOBI Conference*, 2020, Munich, Germany (postponed).

[11] Pipkorn, B., Alvarez, V., Fahlstedt, M., Lundin, L. (2020) Head Injury Risks and Countermeasures for a Bicyclist Impacted by a Passenger Vehicle. *Proceedings of IRCOBI Conference*, 2020, Munich, Germany (postponed).

[12] Versace, J. (1971) A Review of the Severity Index. *Proceedings of 15th Stapp Car Crash Conference*, 1971, Warrendale.

[13] Newman, J. A., Shewchenko, N., Welbourne, E. (2000) A proposed new biomechanical head injury assessment function - the maximum power index. *Stapp Car Crash Journal*, **44**: p.215–247.

[14] Takhounts, E. G., Craig, M. J., Moorhouse, K., McFadden, J., Hasija, V. (2013) Development of brain injury criteria (BrIC). *Stapp Car Crash Journal*, **57**: pp.243–266.

[15] Takhounts, E. G., Eppinger, R. H., *et al*. (2003) On the Development of the SIMon Finite Element Head Model. *Stapp Car Crash Journal*, **47**: pp.107–133.

[16] Kleiven, S. (2013) Why Most Traumatic Brain Injuries are Not Caused by Linear Acceleration but Skull Fractures are. *Frontiers in Bioengineering and Biotechnology*, **1**: p.15.

[17] Krundaeva, A., De Bruyne, G., Gagliardi, F., Van Paepegem, W. (2016) Dynamic compressive strength and crushing properties of expanded polystyrene foam for different strain rates and different temperatures. *Polymer Testing*, **55**: pp.61–68.

[18] Croop, B., Lobo, H. (2009) Selecting material models for the simulation of foams in LS-DYNA. *Proceedings of 7th European LS-Dyna Conference*, 2009, Salzburg.

[19] European Committee for Standardization (2012) Helmets for Pedal Cyclists and for Users of Skateboards and Roller Skates. EN1078:2012, 2012.

[20] Cao, K., Wang, Y., Wang, Y. (2014) Experimental investigation and modeling of the tension behavior of polycarbonate with temperature effects from low to high strain rates. *International Journal of Solids and Structures*, **51**(13): pp.2539–2548.

[21] Toyota, "THUMS - Total Human Model for Safety", https://www.toyota.co.jp/thums/. [Accessed: 26 March 2022].

[22] Garman, C. M., Como, S. G., *et al*. (2020) Micro-Mobility Vehicle Dynamics and Rider Kinematics during Electric Scooter Riding. *Proceedings of WCX SAE World Congress Experience*, 2020, Detroit.

[23] Klug, C., Ellway, J. (2021) Euro NCAP, European New Car Assessment Programme. Pedestrian Human Model Certification. Version 3.0.1.

[24] Prasad, P., Mertz, H. J. (1985) The position of the United States delegation to the ISO Working Group 6 on the use of HIC in the automotive environment. *Proceedings of SAE Government/Industry Meeting and Exposition*, 1985, Washington D.C.

[25] Cripton, P. A., Dressler, D. M., Stuart, C. A., Dennison, C. R., Richards, D. (2014) Bicycle helmets are highly effective at preventing head injury during head impact: head-form accelerations and injury criteria for helmeted and unhelmeted impacts. *Accident Analysis & Prevention*, **70**: pp.1–7.

[26] Levadnyi, I., Awrejcewicz, J., Zhang, Y., Goethel, M. F., Gu, Y. (2018) Finite element analysis of impact for helmeted and non-helmeted head. *Journal of Medical and Biological Engineering*, **38**(4): pp.587–595.

[27] Iwamoto, M., Nakahira, Y. (2014) A preliminary study to investigate muscular effects for pedestrian kinematics and injuries using active THUMS. *Proceedings of IRCOBI Conference*, 2014, Berlin, Germany.

[28] Trube, N., Riedel, W., Boljen, M. (2021) How muscle stiffness affects human body model behavior. *BioMedical Engineering OnLine*, **20**(1): pp.1–39.

[29] Klein, H., Jenerowicz, M., Trube, N., Boljen, M. (2020) How to Combine 3D Textile Modeling with Latest Human Body Models. *Advances in Transdisciplinary Engineering*, **11**: pp.166–177.

[30] Montgomery, S. M., Hilborn, H., *et al.* (2021) The 3D printing and modeling of functionally graded Kelvin foams for controlling crushing performance. *Extreme Mechanics Letters*, **46**: p.101323.

VIII. APPENDIX

A. Injury criteria

TABLE IV
INJURY CRITERIA

Criteria	Equation	Constants
HIC [12]	$HIC = \max\left[\frac{1}{t_2 - t_1}\int_{t_1}^{t_2} a(t)dt\right]^{2.5}(t_2 - t_1)$	-
BrIC [14]	$BrIC = \sqrt{\left(\frac{\omega_{\max\_x}}{\omega_{xc}}\right)^2 + \left(\frac{\omega_{\max\_y}}{\omega_{yc}}\right)^2 + \left(\frac{\omega_{\max\_z}}{\omega_{zc}}\right)^2}$	ω_{xc} = 66.3 rad/s ω_{yc} = 53.8 rad/s ω_{zc} = 41.5 rad/s

B. Helmet modelling and erosion

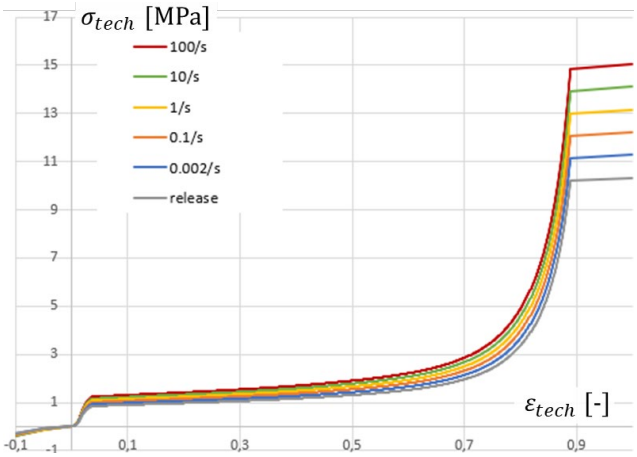

Fig. 17. Stress strain curves dependent on strain rate as input for the foam material model

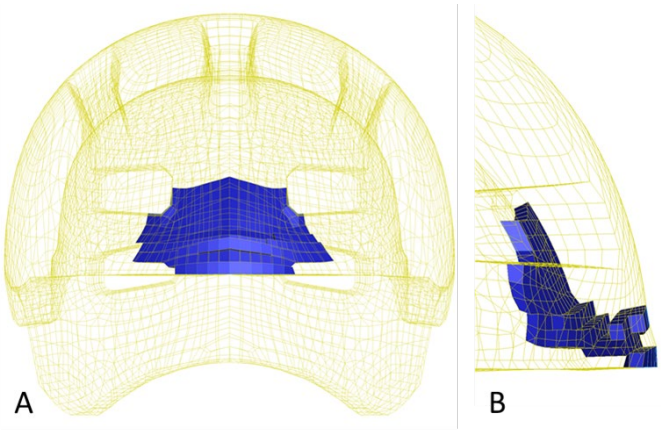

Fig. 18. Eroded region (blue) of helmet (60_10_w): 1.7% elements have been deleted (A – Front, B – Side).

Fig. 19. Damaged helmet after drop tower impact (alpha = 15°, beta = 0°)

Figure 18 illustrates a typical case of eroded helmet elements, in which a small area of the innermost element layer has been eroded and the eroded elements propagate forward in a crack-like pattern. Figure 19 illustrates a damaged helmet after a drop tower impact, showing that cracking is to be expected to some extent.

C. Kinetic energy, acceleration and velocity profiles

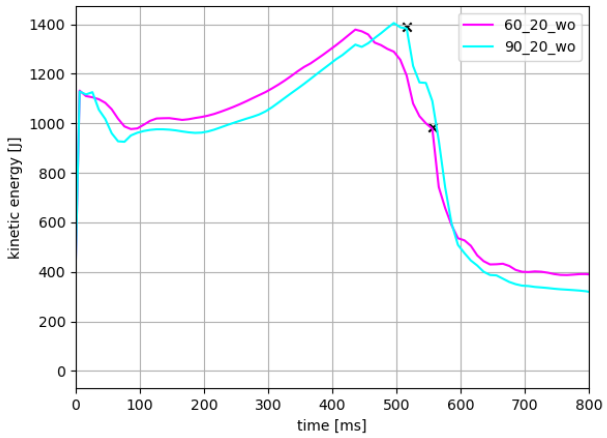

Fig. 20. Kinetic energy of THUMS without helmet, a scooter velocity of 20 km/h and an angle of 60° and 90°. Symbol x indicates first contact of the head with the ground.

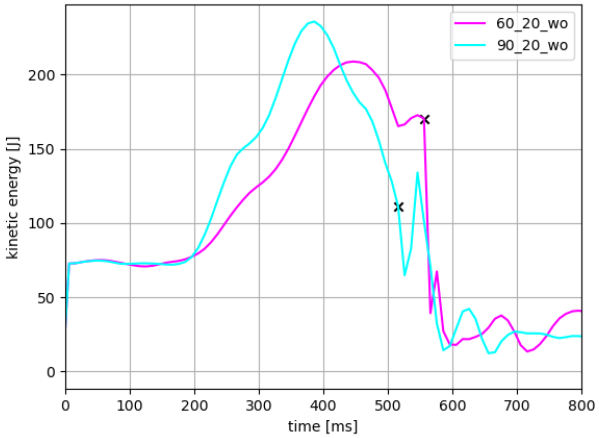

Fig. 21. Kinetic energy of head without helmet, a scooter velocity of 20 km/h and an angle of 60° and 90°. Symbol x indicates first contact of the head with the ground.

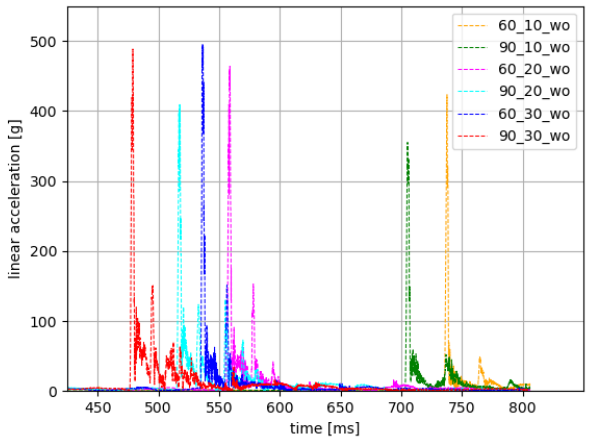

Fig. 22. Linear resultant acceleration in HCG without helmet

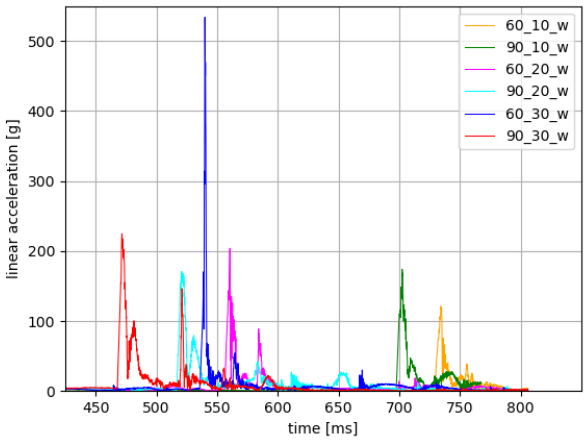

Fig. 23. Linear resultant acceleration in HCG with helmet

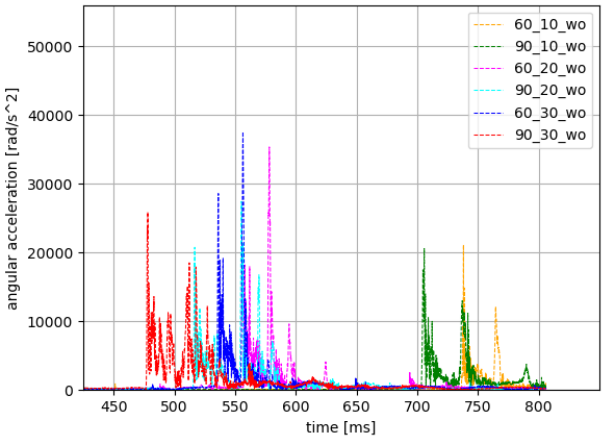

Fig. 24. Angular resultant acceleration in HCG without helmet

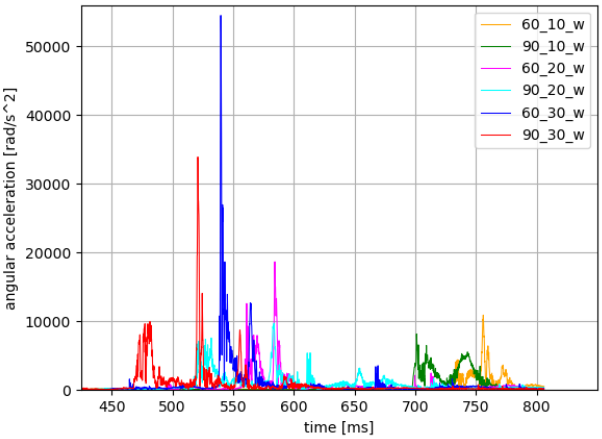

Fig. 25. Angular resultant acceleration in HCG with helmet

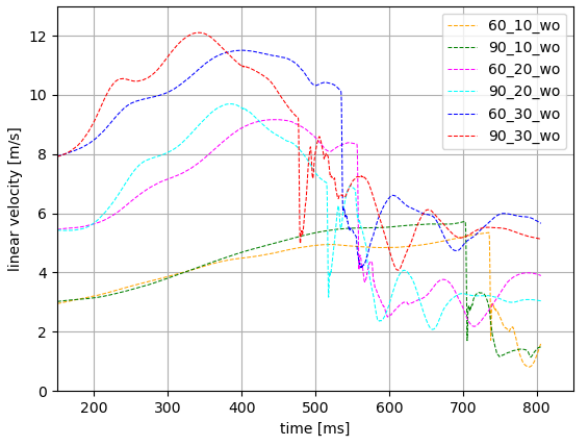

Fig. 26. Linear resultant velocity in HCG without helmet

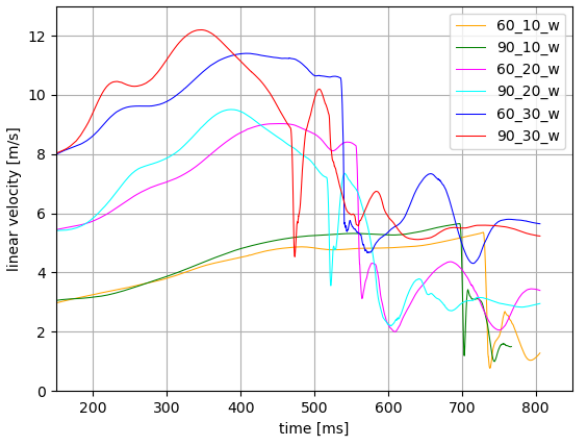

Fig. 27. Linear resultant velocity in HCG with helmet

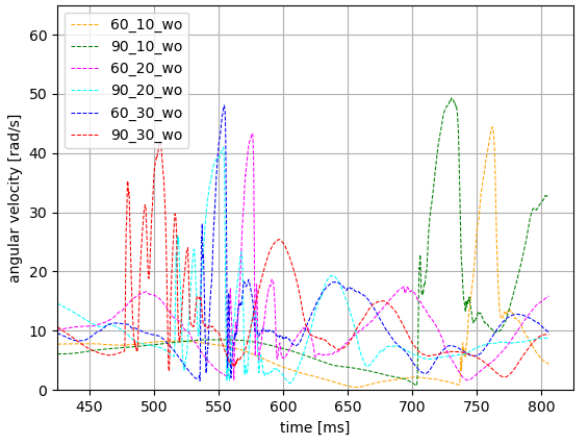

Fig. 28. Angular resultant velocity in HCG without helmet

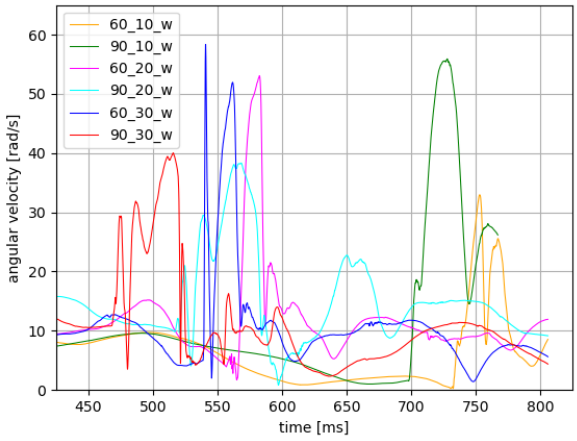

Fig. 29. Angular resultant velocity in HCG with helmet